# Simulation of Muscle Loading in Two Activities with Finite Element Analysis

By:

**Muhammad Haziq Bin Abu Bakar**

(Matrix no.: 120399)

Supervisor:

**Dr. Mohamad Ikhwan Zaini Bin Ridzwan**

This dissertation is submitted to
Universiti Sains Malaysia
As part of the fulfillment of the requirement to graduate with honors degree in
**BACHELOR OF ENGINEERING (MECHANICAL ENGINEERING)**

School of Mechanical Engineering
Engineering Campus
Universiti Sains Malaysia

# DECLARATION

I hereby declare that the work reported in this thesis is the result of my own investigation and that no part of the thesis has been plagiarized from external sources. Materials taken from other sources are duly acknowledgements by giving explicit references.

Signature:

Name of student: MUHAMMAD HAZIQ BIN ABU BAKAR

Matrix number: 120399

Date: June 7$^{th}$ 2017

## ACKNOWLEDGEMENT

First and foremost, I would like to express my deepest gratitude to my supervisor, Dr. Mohamad Ikhwan Zaini Bin Ridzwan for guiding and helping me in completing the project. I am truly indebted and thankful to him for all the time he spent sharing his expertise, valuable guidance and encouragement to me. He constantly assisted me in the right direction whenever he thought I needed it.

I would also want to extend my acknowledgement to Prof. Dr. Zainal Alimuddin Zainal Alauddin, the Dean of School of Mechanical Engineering, University Science Malaysia for providing the facility that is crucial in finishing the project.

Next, I would like to express my appreciation to my parents whom always supported and believed in me. Their encouragement is the main drive of this accomplishment.

Finally, my gratitude goes to all of my colleagues and technical staffs in School of Mechanical Engineering, USM that had helped me completing the project. Thank you.

# TABLE OF CONTENTS


**TABLE OF CONTENTS** 3

**LIST OF FIGURES** i

**LIST OF TABLES** iii

**LIST OF ABBREVIATIONS** iv

**ABSTRAK** v

**ABSTRACT** vi

**CHAPTER ONE: INTRODUCTION** 1

1.1 Research Background 1

1.2 Objectives 2

1.3 Structure of Thesis 2

**CHAPTER TWO: LITERATURE REVIEWS** 3

2.1 Hip Anatomy 3

2.1.1 Femur Anatomy 4

2.2 Muscles around femoral bone 5

2.3 Bone Material Properties 9

2.3.1 Hounsfield Unit (HU), Modulus of Elasticity and Density relationship 9

2.4 Loading and Boundary Conditions 10

**CHAPTER THREE: RESEARCH METHODOLOGY** 13

3.1 3-D Model Generation 13

3.2 Reconstruction of 3-D Model 15

3.3 Meshing of 3-D model 15

3.4 Material Properties Assignment 16

3.5 Mesh Convergence Study 17

3.6 FE analysis 17

3.6.1 Regions of Interests (ROIs) 19

3.6.2 Strain Criterion 20

**CHAPTER FOUR: RESULTS AND DISCUSSIONS** 21

4.1 Walking Condition 21

4.1.1 ROI – Femoral neck 21

4.1.2 ROI – Femoral shaft 21

4.2 Stair climbing condition 25

4.2.1 ROI – Femoral neck 25

4.2.2 ROI – femoral shaft 25

**CHAPTER FIVE: CONCLUSION** 35

**REFERENCES** ____ **36**

**APPENDICES** ____ **38**

## LIST OF FIGURES

Figure 2. 1. Hip anatomy configuration [7] ........................................................................3
Figure 2. 2. Femoral bone configuration [10]........................................................................4
Figure 2. 3. Femoral bone muscles configuration [10] ..........................................................6
Figure 2. 4. Location and direction of the forces acting on the femur [6]..............................11
Figure 2. 5. Stance phase of walking [21] ............................................................................11
Figure 2. 6. Stance phase of stairs climbing [21].................................................................12
Figure 2. 4. Location and direction of the forces acting on the femur [6]..............................18

Figure 3. 1. Overview of the flow of the research methodology ______________________ 13
Figure 3. 2. All the desired regions were selected using fill cavity option in Mimics interface. (a) represents transverse plane, (b) coronal plane and (c) sagittal plane ________________ 14
Figure 3. 3. Initial condition (left) and the after-smooth and remesh condition of 3-D model of the femoral bone_______________________________________________________ 15
Figure 3. 4. Mesh size of (a) 2 mm; (b) 2.5 mm; (c) 3 mm; (d) 4 mm. different mesh size was done to perform the mesh convergence study to determine the most suitable mesh size for the real analysis ______________________________________________________ 16
Figure 3. 5. Material distribution of the femoral bone generated in BONEMAT _________ 16
Figure 3. 6. Convergence of strain values as the mesh size reduced ___________________ 17
Figure 3. 7. Elements selections for (a) medial and lateral quadrants, (b) anterior quadrant and (c) posterior quadrant for femoral neck ___________________________________ 20
Figure 3. 8. Elements selections for (a) medial and lateral quadrants, (b) anterior quadrant, and (c) posterior quadrant for femoral shaft ROI _________________________________ 20

Figure 4. 1. Maximum and minimum principal strain for inferior (top left), superior (bottom left), anterior (top right) and posterior (bottom right) quadrants for femoral neck region (walking condition) ________________________________________________ 23
Figure 4. 2. Maximum and minimum principal strain for medial (top left), lateral (bottom left), anterior (top right) and posterior (bottom right) quadrants for femoral shaft region (walking condition)____________________________________________________ 24
Figure 4. 3. Maximum and minimum principal strain for inferior (top left), superior (bottom left), anterior (top right) and posterior (bottom right) quadrants for femoral neck region___ 26
Figure 4. 4. Maximum and minimum principal strain for medial (top left), lateral (bottom left), anterior (top right) and posterior (bottom right) quadrants for femoral shaft region _______ 27
Figure 4. 5. Averaged strain values for each quadrant; inferior (top left), superior (bottom left), anterior (top right) and posterior (bottom right) for femoral neck region (walking condition)____________________________________________________ 31
Figure 4. 6. Averaged strain values for each quadrant; inferior (top left), superior (bottom left), anterior (top right) and posterior (bottom right) for femoral shaft region (walking condition)____________________________________________________ 32
Figure 4. 7. Averaged strain values for each quadrant; inferior (top left), superior (bottom left), anterior (top right) and posterior (bottom right) for femoral neck region (stairs climbing condition)____________________________________________________ 33

Figure 4. 8. Averaged strain values for each quadrant; inferior (top left), superior (bottom left), anterior (top right) and posterior (bottom right) for femoral neck region (walking condition) 34

Figure A. 1. 1st principal elastic strain for walking condition case 1 ......................................38
Figure A. 2. 1st principal elastic strain for walking condition case 2 ......................................38
Figure A. 3. 1st principal elastic strain for walking condition case 3 ......................................39
Figure A. 4. 1st principal elastic strain for stairs climbing condition case 1............................39
Figure A. 5. 1st principal elastic strain for stairs climbing condition case 2............................40
Figure A. 6. 1st principal elastic strain for stairs climbing condition case 3............................40
Figure A. 7. 1st principal elastic strain for stairs climbing condition case 4............................40

# LIST OF TABLES

Table 2. 1. Muscles that attached to the femoral bone ........................................................... 5
Table 2. 2. Classification or grouping of muscles [6] ............................................................ 7
Table 2. 3. Muscles that used in this study are illustrated in shaded grey area ........................ 8
Table 2. 4. Loading condition (in percentage of BW) for walking with BW of 836N [6] ....... 10
Table 2. 5. Loading condition (in percentage BW) for stair climbing with BW of 836N [6] .. 10
Table 2. 4. Loading condition (in percentage of BW) for walking with BW of 836N [6] ....... 18
Table 2. 5. Loading condition (in percentage BW) for stair climbing with BW of 836N [6] .. 18

Table 3. 1. Categorization of cases in FE analysis for walking condition .............................. 19
Table 3. 2. Categorization of cases in FE analysis for stair climbing condition ...................... 19

## LIST OF ABBREVIATIONS

| | | |
|---|---|---|
| BMD | – | Bone Mineral Density |
| FE | – | Finite Element |
| HU | – | Hounsfield Unit |
| CT | – | Computed Tomography |
| $\rho_{app}$ | – | Apparent Density |
| E | – | Modulus of Elasticity |
| BW | – | Bodyweight |
| ROI | – | Region of Interest |

# ABSTRAK

Tidak dinafikan lagi bahawa otot memainkan peranan yang amat penting dalam memanipulasi agihan terikan tulang femoral (tulang pada lokasi peha). Walau bagaimanapun, signifikasi kesannya belum dapat diukur secara jelas dalam mana-mana kajian. Oleh itu, kajian ini dijalankan bagi menentukan signifikasi daya otot pada aktiviti harian, iaitu aktiviti berjalan dan menaiki tangga serta menentukan otot yang mana (abductor, vastus lateralis dan medialis) penting dalam aktiviti-aktiviti tersebut. Model 3-D tulang femoral dibina daripada set data CT dan dikenakan daya yang bersesuaian, bergantung kepada simulasi aktiviti yang dikaji. Terikan maksimum dan minimum hasil daripada daya yang dikenakan di kawasan kepentingan (ROI) (leher tulang femoral dan batang tulang femoral) diukur dan direkodkan. Hasil simulasi menunjukkan bahawa, pada aktiviti berjalan, otot yang aktif (abductor dan vastus lateralis) memberi kesan yang ketara dalam mengubah agihan terikan pada bahagian leher tulang femoral (95%, menurut student t-test). Pada aktiviti menaiki tangga, sumbangan otot (abductor, vastus lateralis dan medialis) juga menghasilkan keputusan yang ketara terutama pada bahagian leher tulang femoral femoral (95%, menurut student t-test). Oleh itu, otot sesungguhnya menyumbang dengan ketara pada analisis yang dilakukan dan ia sememangnya perlu bagi memperolehi keputusan yang lebih tepat dan lebih dipercayai.

## ABSTRACT

No doubt that muscle play important role in manipulating the strain distribution of the femoral bone. However, the significances are yet to be measured clearly in any literature. This study is conducted to determine the significances of muscles forces in walking and stairs climbing activities and establish which muscle (abductor, vastus lateralis or vastus medialis) is important in those activities. 3-D model of the femoral bone was constructed from CT datasets and appropriate loading conditions were subjected to it. The maximum and minimum strains at two regions of interest (femoral neck and femoral shaft) were recorded. The FE outcomes showed that, for walking activity, muscles activation (abductor and vastus lateralis) contributed to significant changes in strain distribution (95%, based on student t-test) in femoral neck region. In stairs climbing activity, contribution of muscles (abductor, vastus lateralis and medialis) is also notable in femoral neck region (95%, based on student t-test). Hence, muscles is indeed contributed significantly and required to be incorporated in the analysis.

# CHAPTER ONE: INTRODUCTION

## 1.1 Research Background

There are many diseases that affect the lower extremities of a human anatomy. Many researches had been performed in order to predict and prevent the risk of having those diseases. One of the diseases is Osteoporosis, a weakening in bone's strength condition. It is a condition where the Bone Mineral Density (BMD) will drastically reduce, deteriorating bones' microstructural characteristics as a result of excessive bone resorption followed by insufficient bone formation during remodeling [1]. Many studies in regards to the bone strength had been conducted, whether it is experimentally or through Finite Element (FE) method. Edwards, Miller [2] conducted a research on strain distribution during walking, predicted with muscle forces. But their focus are more on comparing two different method instead of highlighting the significance of muscle contribution. The experimental method such as in vivo measurements of muscle forces are mostly highly invasive [3]. Another approach, the FE method, is inexpensive, non-invasive, and capable to incorporate the geometry and shape, and the mechanics of bone into one single model [4]. Another upper hand FE method has towards experimental procedure is the simplicity in subjecting the loading condition to the model. Even though the mechanisms of the functional adaptation of the muscle are not fully understood, FE method provides a precise tool for analysis of the strain distribution in the bone [3]. Many experimental studies concerning bone strength neglected the muscle activation in their analysis. Kumar, Tandon [5] deduced, that the muscle forces consideration will reduce the stress up to 30%. In other study, the inclusion of muscle forces reduced the peak strains at the femoral neck significantly [6]. Hence, muscle contribution should not be taken lightly as it could produce inaccurate and invalid results. Nevertheless, the significances of muscles forces and which muscle should be included or excluded in the analysis has to be determined so that the simplification of the model, whether it is experimental or simulation will not jeopardize the outcome.

## 1.2 Objectives

1. To investigate a significant contribution of muscles' forces (magnitude and direction) to femoral bone strength based on two major activities, walking and stairs climbing.
2. To determine which muscles would have significant role when analyzing a walking and stairs climbing activities.

## 1.3 Structure of Thesis

The thesis is divided into five chapters. Chapter One (Introduction), introduces the research background, problem statements and the objectives of the study. Chapter Two (literature review), discusses the literature background in regards of the study, such as femur anatomy, muscle categorization, material properties of the bone and loading conditions. Chapter Three (Methodology), explains the procedure of the study from the beginning (generating 3-D model of femoral bone) until the extraction of data from the FE simulation. Chapter Four (Results and Discussions), contains all the raw and analyzed data and discussing the patterns and significances of the results obtained. Chapter Six (Conclusion), deducing whether the objectives are accomplished or not.

# CHAPTER TWO: LITERATURE REVIEWS

## 2.1 Hip Anatomy

Hip is generally a synovial joint of ball and socket, where the ‘ball’ is the femoral head and the ‘socket’ is the acetabulum [7]. It is the largest ball-and-socket joint in the human body [8]. The configuration of hip joint consists of pelvis, femur and acetabulum (Figure 2.1) [7].

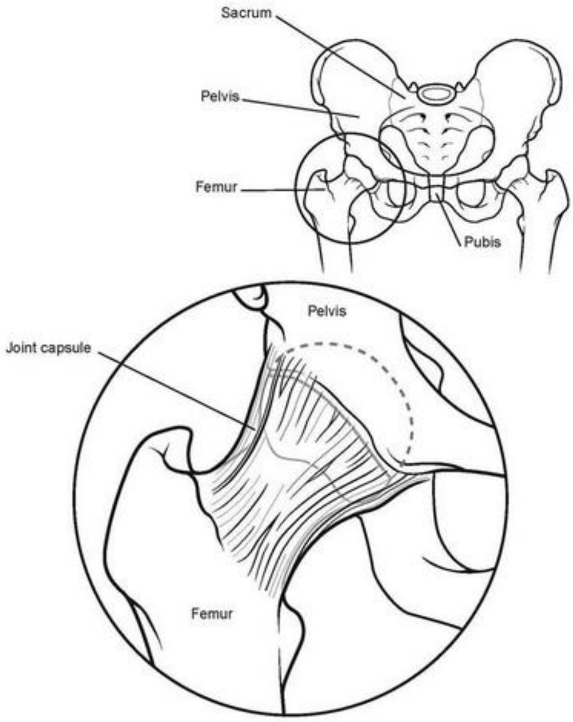


Figure 2. 1. Hip anatomy configuration [7]

The joint capsule (Figure 2.1) is a articular cartilage with thickness of a quarter inch that covers the femoral head and the acetabulum [9]. The synovial membrane produced lubricant to smoothen the joint, making the bone movement easily and painless [9]. A person can moves and performs daily activities due to a healthy hip that is able to support the weight of the person.

### 2.1.1 Femur Anatomy

Femur is the longest and heaviest bone in the human body, which consists of superior region (proximal end), shaft, and inferior region (distal end) [7]. The superior region or the upper end region consists of the head, neck, trochanter (greater and lesser trochanter) and intertrochanteric (intertrochanteric line and crest) (Figure 2.3) [3]. The lower end (inferior region) consists of two large condyles (medial and lateral condyle) and the shaft connects the two regions [3].

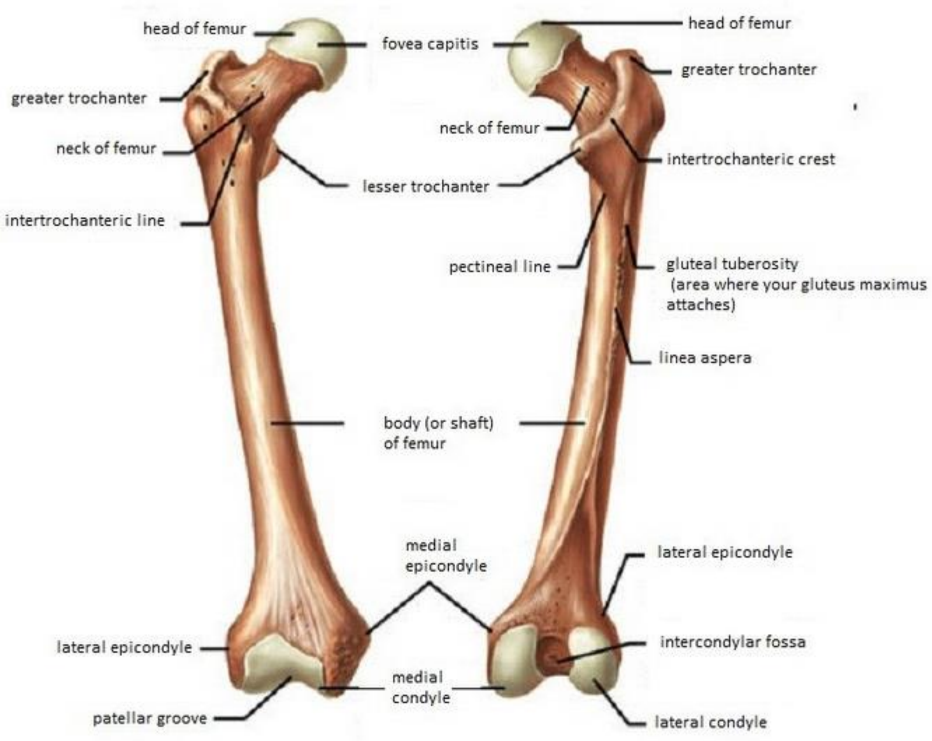


Figure 2. 2. Femoral bone configuration [10]

## 2.2 Muscles around femoral bone

The total muscles that either originate from or insert onto the femur are 22. Table 2.1 below tabulated all the 22 muscles and their attachment location.

Table 2. 1. Muscles that attached to the femoral bone

| Muscle | Direction | Attachment |
|---|---|---|
| Iliacus muscle | Insertion | Lesser trochanter |
| Psoas major muscle | Insertion | |
| Gluteus maximus muscle | Insertion | Gluteal tuberosity |
| Gluteus medius muscle | Insertion | Lateral surface of greater trochanter |
| Gluteus minimus muscle | Insertion | Forefront of greater trochanter |
| Piriformis muscle | Insertion | Superior boundary of greater trochanter |
| Gemellus superior muscle | Insertion | Upper edge of Obturator internus's tendon |
| Obturator internus muscle | Insertion | Medial surface of greater trochanter |
| Gemellus inferior muscle | Insertion | Lower edge of Obturator internus's tendon |
| Quadratus femoris muscle | Insertion | Intertrochanteric crest |
| Obturator externus muscle | Insertion | Trochanteric fossa |
| Pectineus muscle | Insertion | Pectineal line |
| Adductor longus muscle | Insertion | Medial ridge of linea aspera |
| Adductor longus muscle | Insertion | Medial ridge of linea aspera |
| Adductor brevis muscle | Insertion | Medial ridge of linea aspera |
| Adductor magnus muscle | Insertion | Medial ridge of linea aspera and the adductor tubercle |
| Vastus lateralis muscle | Origin | Greater trochanter and lateral ridge of linea aspera |
| Vastus intermedius muscle | Origin | Front and lateral surface of femur |
| Vastus medialis muscle | Origin | Distal part of intertrochanteric line and medial ridge of linea aspera |
| Short head of biceps femoris | Origin | Lateral ridge of linea aspera |
| Popliteus muscle | Origin | Under the lateral epicondyle |
| Gastrocnemius muscle | Origin | Behind the adductor tubercle, over the lateral epicondyle and the popliteal facies |
| Plantaris muscle | Origin | Over the lateral condyle |

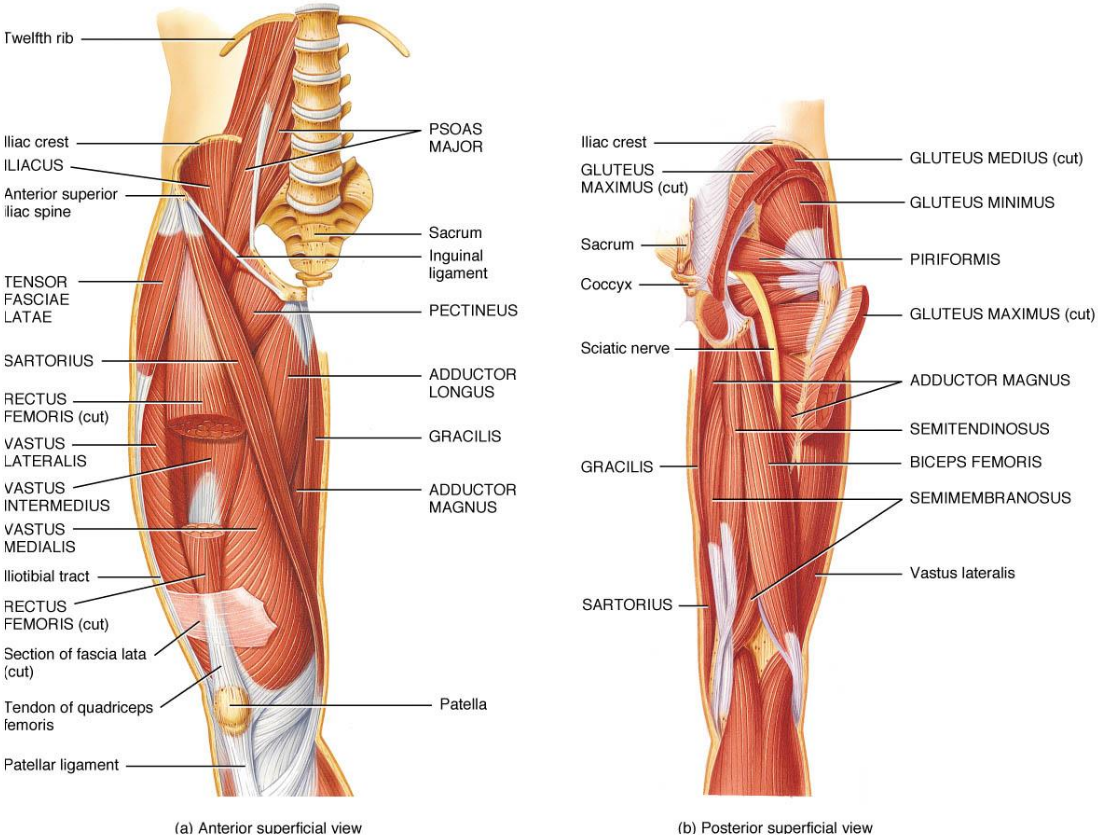


Figure 2. 3. Femoral bone muscles configuration [10]

However, in this study, the muscles that will be taken into consideration are the ones that active during performing walking and climbing stairs activities. Morgan, Bayraktar [11] study on muscle loading at the hip joint will be the main reference, in term of the muscles activation during walking and climbing stairs conditions. Their work simplified the musculoskeletal system by focusing on the ‘single joint muscles’, muscles that solely span the hip joint [11]. Muscle with identical purpose was grouped together, producing group of muscle as tabulated in table 2.2.

Table 2. 2. Classification or grouping of muscles [6]

| **Complex muscle** | **Simplfied muscle** |
|---|---|
| Gluteus medius | Abductor |
| Gluteus minimus | |
| Gluteus maximum | |
| Adductor magnus | Adductor |
| Adductor longus | |
| Adductor brevis | |
| Ilio-tibial tract | Unchanged |
| Tensor fascia latae | unchanged |

For ‘two joint muscles’, muscles that span both the hip and knee joint, they also contribute to the hip contact force and are crucial for gaining physiological-like loading conditions. Nonetheless, these muscles do not possess attachment sites at the proximal femur, thus deployed no direct forces on the bone [11]. The ‘two joint muscles’ include:

- Bicep femoris
- Semitendinosous
- Semimembranosous
- Rectus femoris
- Gracilis
- Sartorius

The simplification of muscles was further implemented by sequential removal of muscles with small forces, up to a point where unphysiological hip joint loading was calculated [11]. The list of muscles that had been removed are as follow:

- Iliacus
- Psoas major
- Pectineus
- Gmellus inferior & superior
- Obturator externus & internus
- Piriformis

Table 2. 3. Muscles that used in this study are illustrated in shaded grey area

| Muscle | Direction | Attachment | Status |
|---|---|---|---|
| Iliacus muscle | Insertion | Lesser trochanter | Removed |
| Psoas major muscle | Insertion | | |
| Gluteus maximus muscle | Insertion | Gluteal tuberosity | Included as Abductor |
| Gluteus medius muscle | Insertion | Lateral surface of greater trochanter | |
| Gluteus minimus muscle | Insertion | Forefront of greater trochanter | |
| Piriformis muscle | Insertion | Superior boundary of greater trochanter | Removed |
| Gemellus superior muscle | Insertion | Upper edge of Obturator internus's tendon | |
| Obturator internus muscle | Insertion | Medial surface of greater trochanter | |
| Gemellus inferior muscle | Insertion | Lower edge of Obturator internus's tendon | |
| Quadratus femoris muscle | Insertion | Intertrochanteric crest | |
| Obturator externus muscle | Insertion | Trochanteric fossa | |
| Pectineus muscle | Insertion | Pectineal line | |
| Adductor longus muscle | Insertion | Medial ridge of linea aspera | Included as Adductor |
| Adductor brevis muscle | Insertion | Medial ridge of linea aspera | |
| Adductor magnus muscle | Insertion | Medial ridge of linea aspera and the adductor tubercle | |

| | | | |
|---|---|---|---|
| Vastus lateralis muscle | Origin | Greater trochanter and lateral ridge of linea aspera | Included |
| Vastus intermedius muscle | Origin | Front and lateral surface of femur | Removed |
| Vastus medialis muscle | Origin | Distal part of intertrochanteric line and medial ridge of linea aspera | Included |
| Short head of biceps femoris | Origin | Lateral ridge of linea aspera | Removed |
| Popliteus muscle | Origin | Under the lateral epicondyle | |
| Gastrocnemius muscle | Origin | Behind the adductor tubercle, over the lateral epicondyle and the popliteal facies | |
| Plantaris muscle | Origin | Over the lateral condyle | |

## 2.3 Bone Material Properties

To perform FE analysis and obtaining accurate results, the assignment of mechanical properties of the model is pivotal [12]. In real condition, bone exhibits heterogeneous anisotropic behavior due to its complex microarchitecture [13]. However, it is extremely difficult to model the anisotropic mode, especially when modeling for Osteoporotic femora [4]. Many works such as Jiang, Missoum [14], Ali, Cristofolini [15], and Tsouknidas, Anagnostidis [1] performed their FE analysis by assuming the bone properties to behave isotropically. Heller, Bergmann [6] in their study too, carry out FE analysis using isotropic heterogeneous bone properties, claiming that it is sufficiently accurate and capable to produce realistic strain distributions. The material mapping of the bone relies on three elements, namely Hounsfield Unit (HU), apparent density, $\rho_{app}$ and modulus of elasticity.

### 2.3.1 Hounsfield Unit (HU), Modulus of Elasticity and Density relationship

Hounsfield unit was introduced by Sir Godfrey Newbold Hounsfield, where he tried to quantify the amount of X-rays that pass through or absorbed by tissues [16]. HU scale is used to express the CT number in a comparable form. HU maximum value of a bone (cortical region) was corresponding to the maximum $\rho_{app}$ [17]. Apparent density, $\rho_{app}$ $(g/cm^3)$ is the ratio of hydrated tissue mass to total specimen volume [18]. Many studies had been done in determining the relationship of density and modulus of elasticity of the bone, and for this study, the following relation will be used [18]:

$$E = 6850\,\rho_{app}^{1.49} \qquad (2.1)$$

This relation had been used in many other works that performed FE analysis of the femoral bone [2, 6, 15, 19] with Poisson's ratio of 0.3.

## 2.4 Loading and Boundary Conditions

For this study, the activities that will be simulated are walking and climbing stairs. These conditions were chosen because it is a typical activity in daily life and contains larger data collection compared to activities such as falling and stumbling [20]. On top of that, these activities are clinical relevant to femoral fractures [20], hence the data that will be obtain can be of benefit.

The study by Morgan, Bayraktar [11] will be the primary reference in deciding the loading conditions for both activities. Their findings [11], as tabulated in Table 2.4 and Table 2.5, shows strong activities of the muscles, which could lead to overestimation of results if the analysis would only considered the hip joint force. Figure 2.4 represents the acting point and direction of the forces.

Table 2. 4. Loading condition (in percentage of BW) for walking with BW of 836N [6]

| **Force** | **x** | **y** | **z** | **Act at point** |
|---|---|---|---|---|
| Hip Contact | -54.0 | 32.8 | -229.2 | P0 |
| Abductor | 58.0 | 12.8 | -78.2 | P1 |
| Vastus Lateralis | -0.9 | -18.5 | -92.9 | P2 |

Table 2. 5. Loading condition (in percentage BW) for stair climbing with BW of 836N [6]

| **Force** | **x** | **y** | **z** | **Act at point** |
|---|---|---|---|---|
| Hip Contact | -59.3 | 60.6 | -236.3 | P0 |
| Abductor | 70.1 | -28.8 | 84.9 | P1 |
| Vastus Lateralis | -2.2 | -22.4 | -135.1 | P2 |
| Vastus Medialis | -8.8 | -39.6 | -267.1 | P3 |

Martelli, Pivonka [21] when performing FE analysis for walking and stair climbing conditions, constrained the distal femur kinematically. Hence, this approach will be taken in this study when simulating those activities.

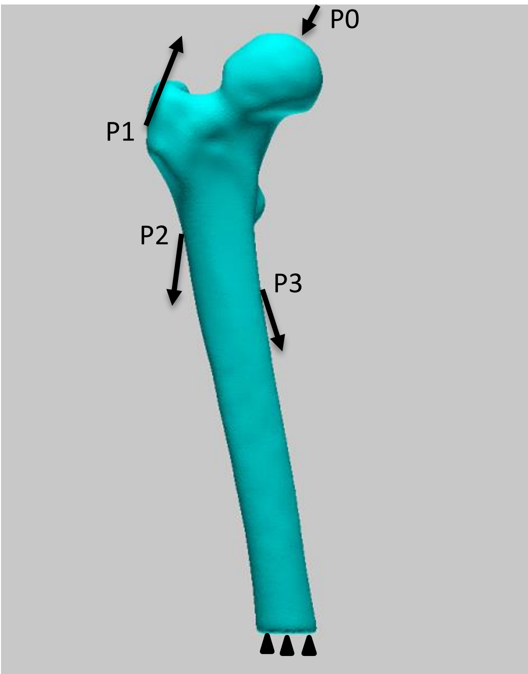


Figure 2. 4. Location and direction of the forces acting on the femur [6]

The forces tabulated in Table 2.4 and Table 2.5 were derived from the walking (Figure 2.5) and stairs climbing gaits (Figure 2.6) where the forces recorded were at the highest, in the early and late stance phase for both conditions [6].

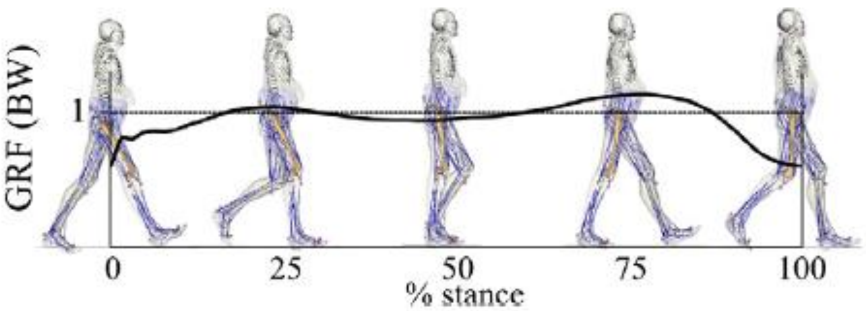


Figure 2. 5. Stance phase of walking [21]

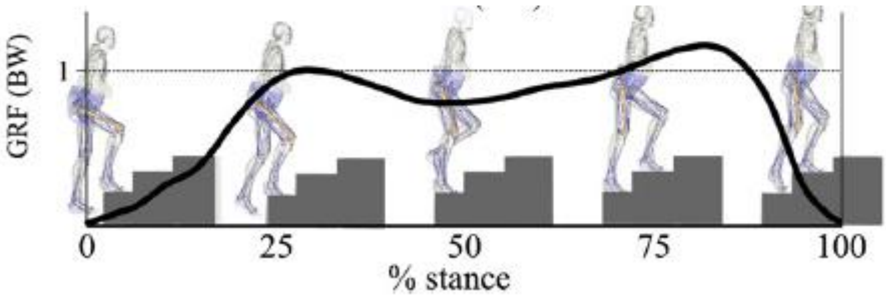


Figure 2. 6. Stance phase of stairs climbing [21]

# CHAPTER THREE: RESEARCH METHODOLOGY

The overview of the research methodology in the study is as illustrated in the figure 3.1.

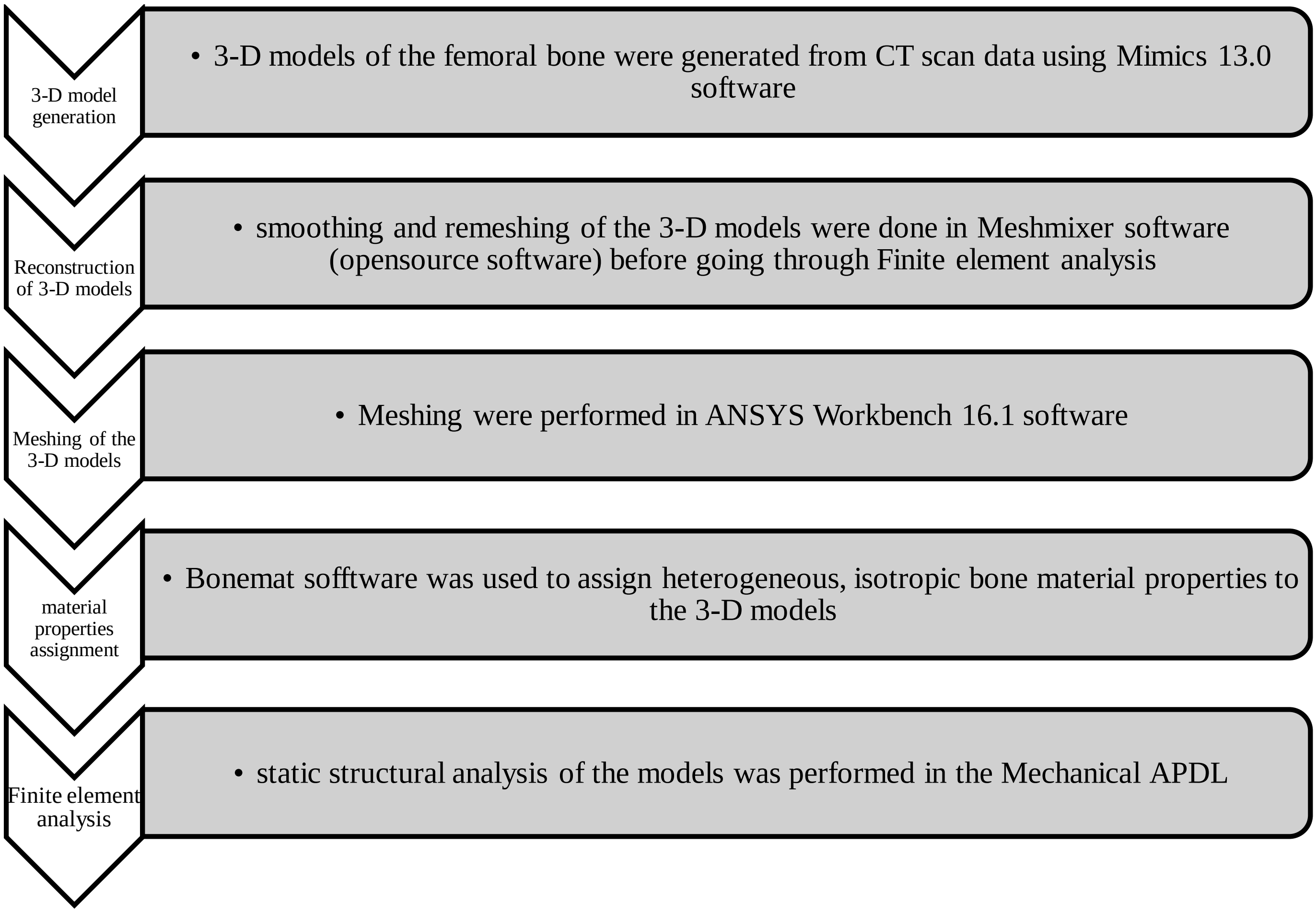


Figure 3. 1. Overview of the flow of the research methodology

## 3.1 3-D Model Generation

Ct datasets of a 79 years old anonymous woman was chosen for this study and was imported into *Mimics 13.0.* the CT contains 394 slices of 512 x 512 matrix in spiral reconstruction mode with a pixel width of 0.96 mm. As shown in figure 3.2, the patient had an implant on her left femur, therefore the right side was selected for the case study.

*Mimics* will automatically generated and created views of the images in sagittal, coronal and transverse planes as shown in Figure 3.2. Next, a new mask was created by choosing *compact bone (adult)* option for the *predefined threshold set*. This option will automatically select region where the Hounsfield Unit (HU) are within the range of 662 and 1988 (range values of HU for compact bone). However, due to high values of HU of the compact bone, there will be regions that were desired such as canceleous bone that are not selected. Thus, a manual editing of the mask was performed to ensure all the required regions were chosen. This part of the procedure was crucial to generate a well-defined 3-D model and assignment of the bone material later on. After finished selecting the regions, as in Figure 3.2, the mask was used to create 3-D model through *calculate 3-D* option. Finally, the model was exported in *.stl* type of file to be imported into *Meshmixer* software for smoothing and remeshing procedure.

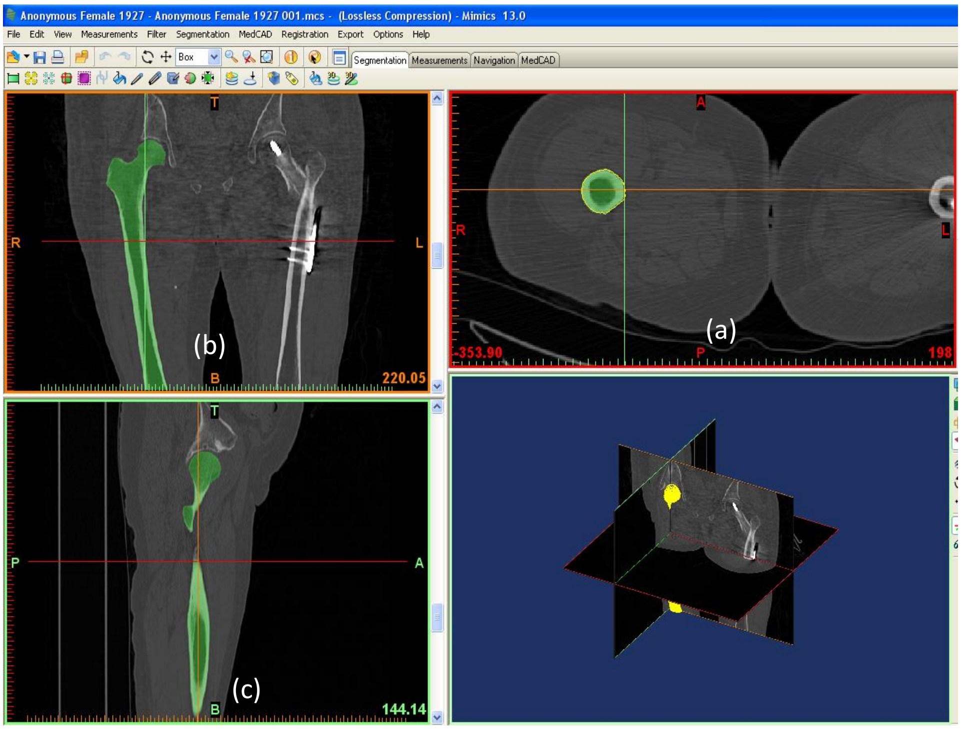


Figure 3. 2. All the desired regions were selected using *fill cavity* option in *Mimics* interface. (a) represents transverse plane, (b) coronal plane and (c) sagittal plane

## 3.2 Reconstruction of 3-D Model

The 3-D model (in *.stl* type file) from *Mimics* was imported into the *Meshmixer* software. *Meshmixer* is an open software created by Autodesk with many tools to work with triangle meshes.

After importing the 3-D model, *smooth* option from the *select* tool was used to create a smoother surface of the bone. The *smoothing scale* was set in the range of four to six, depending on the initial state of the model. Then, *remesh* option, which is also from the *select* tool, was chosen to remesh the triangles of the model to a suitable size. The usual range of edge length was set between one and three. Figure 3.3 shows initial condition (left) of the model and after-smooth and remesh model (right).

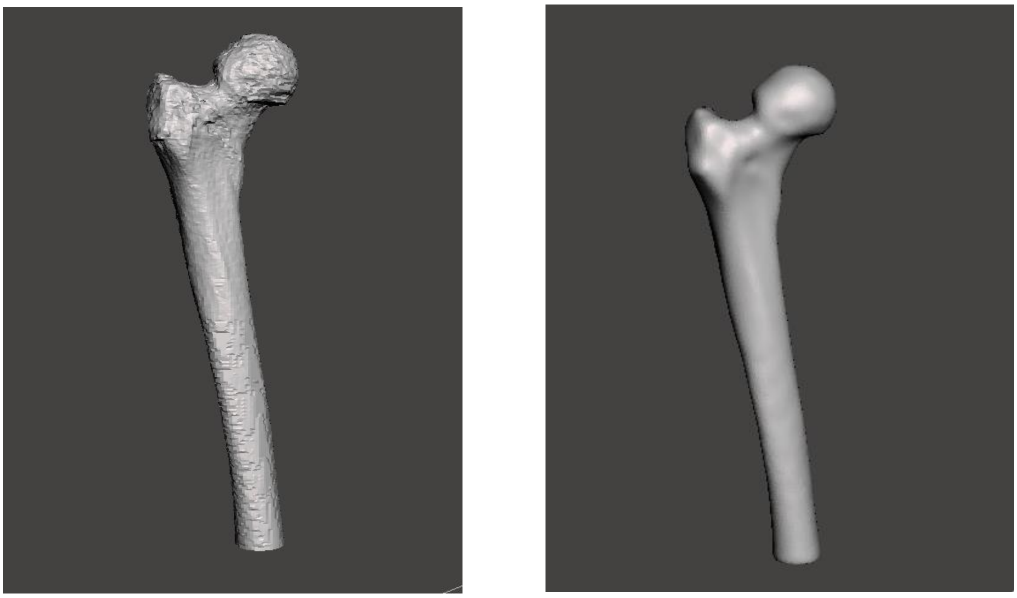

Figure 3. 3. Initial condition (left) and the after-smooth and remesh condition of 3-D model of the femoral bone

## 3.3 Meshing of 3-D model

The meshing process was performed in *ANSYS Workbench 16.1*, through *mesh system* in the *Workbench* toolbox. The femur model's file from the *Meshmixer* was imported and opened in the *SpaceClaim* option. The model was solidified inside it and imported back into *Workbench's mesh system*. The model's mesh was auto-generated with different mesh sizing in order to perform the Mesh Convergence study. *Finite Element Modeler system* was utilized as a file converter, to import the meshed model as *Abaqus's inp.* type file for material mapping in *BONEMAT* software.

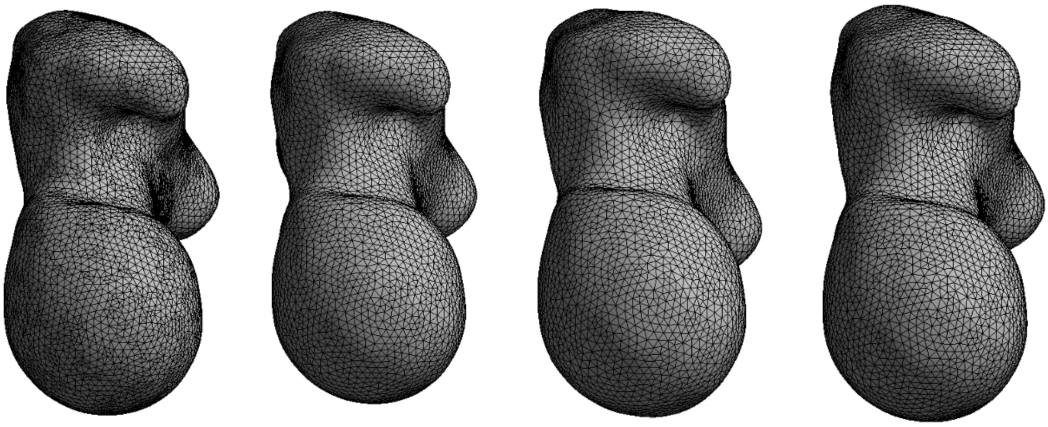

(a) (b) (c) (d)

Figure 3. 4. Mesh size of (a) 2 mm; (b) 2.5 mm; (c) 3 mm; (d) 4 mm. different mesh size was done to perform the mesh convergence study to determine the most suitable mesh size for the real analysis

## 3.4 Material Properties Assignment

The mapping of the material was generated with versatile software, *BONEMAT v3.2.* The software was developed at Institute of Orthopedic Rizzoli, in Bologna, Italy. It is a freeware that maps on a finite element mesh bone elastic properties derived from the CT images.

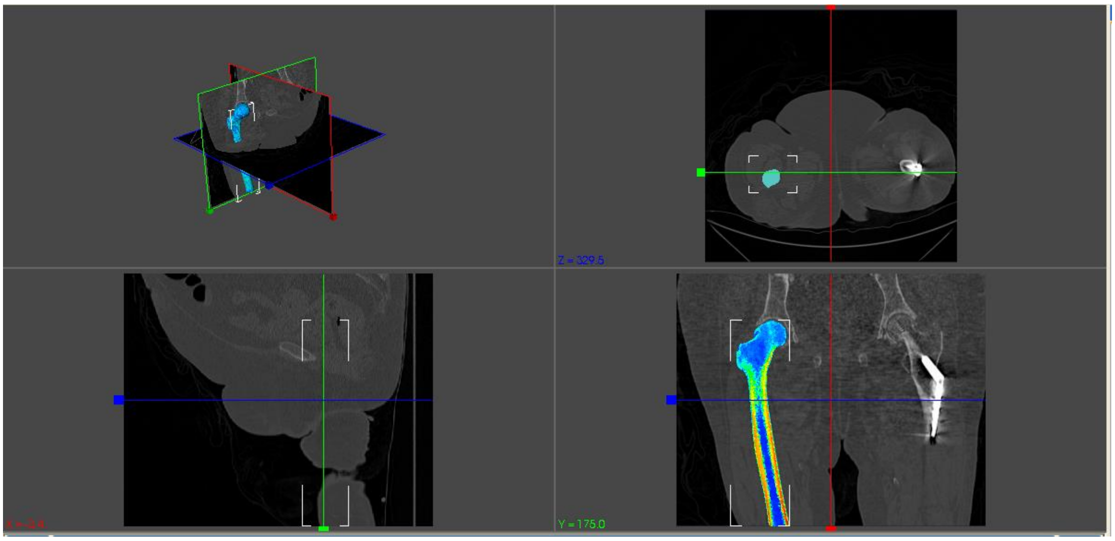

Figure 3. 5. Material distribution of the femoral bone generated in BONEMAT

### 3.5 Mesh Convergence Study

Mesh convergence study was conducted to obtain the most optimized mesh for the FE analysis. Four different sizes of mesh (4, 3, 2.5, and 2 mm) were tested in simple hip joint loading condition (case 1 – walking condition) and the strain values at certain region were recorded and compared. The difference between consequential mesh sizes must be less than 5% for the mesh size to be accepted.

Figure 3.6 is the plotted maximum principal strain value against number of elements for the Mesh Convergence Study. The strain value decreased up to the level where the difference of the value between 3mm (num. of element – 66612) and 2.5mm (num. of element – 107081) mesh size was 3.35%, which was less than 5%. Due to the analysis that was performed was only in static structural, the computational time was not an issue. Therefore, further FE analysis will be conducted by using 2mm mesh size.

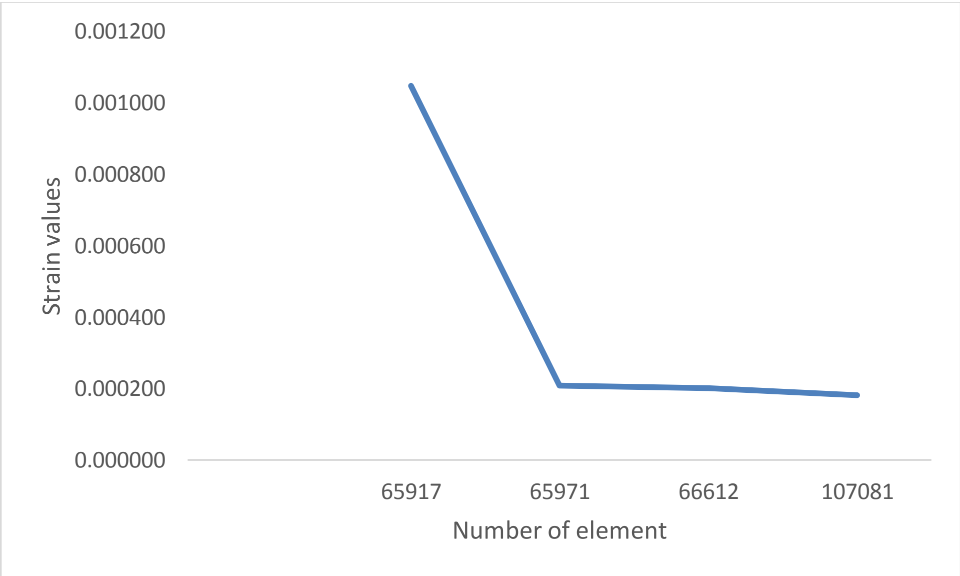


Figure 3. 6. Convergence of strain values as the mesh size reduced

### 3.6 FE analysis

FE analysis of the femoral bone was performed in the *ANSYS Mechanical APDL*. The model that had been assigned with bone's material properties from *BONEMAT* was imported in the *APDL*. Two daily activities (walking and stair climbing) were being analyzed with and without the inclusion of muscles forces. The strain values of the femoral bone were recorded and compared to determine the significances of forces due to the activation of muscles during each activity.

The muscles that were activated during walking and stair climbing were stated in Table 2.4 and 2.5 and the location of the forces are shown in figure 2.4.

Table 2. 6. Loading condition (in percentage of BW) for walking with BW of 836N [6]

| **Force** | **x** | **y** | **z** | **Act at point** |
|---|---|---|---|---|
| Hip Contact | -54.0 | 32.8 | -229.2 | P0 |
| Abductor | 58.0 | 12.8 | -78.2 | P1 |
| Vastus Lateralis | -0.9 | -18.5 | -92.9 | P2 |

Table 2. 7. Loading condition (in percentage BW) for stair climbing with BW of 836N [6]

| **Force** | **x** | **y** | **z** | **Act at point** |
|---|---|---|---|---|
| Hip Contact | -59.3 | 60.6 | -236.3 | P0 |
| Abductor | 70.1 | -28.8 | 84.9 | P1 |
| Vastus Lateralis | -2.2 | -22.4 | -135.1 | P2 |
| Vastus Medialis | -8.8 | -39.6 | -267.1 | P3 |

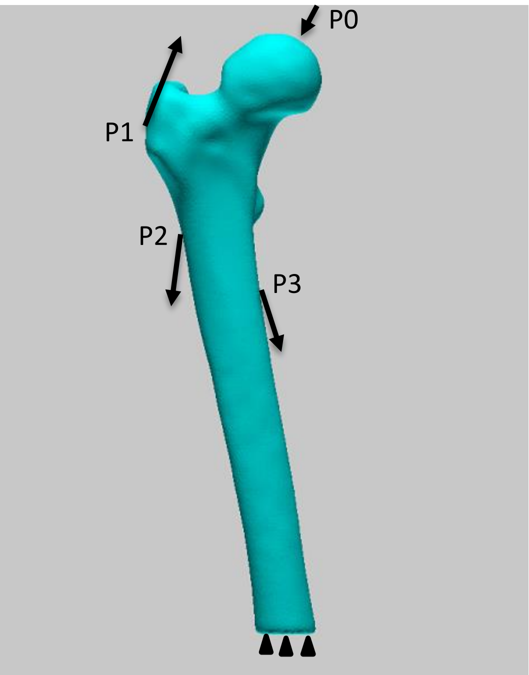


Figure 2. 7. Location and direction of the forces acting on the femur [6]

For walking condition, the simulation was separated in three cases while four cases were performed as tabulated in table 3.1 and 3.2.

Table 3. 1. Categorization of cases in FE analysis for walking condition

| **Walking condition** | | |
|---|---|---|
| **Case** | **Forces involved** | **Location** |
| 1 | Hip force only | P0 |
| 2 | Hip force + Abductors | P1 |
| 3 | Hip force + Abductors + Vastus Lateralis | P2 |

Table 3. 2. Categorization of cases in FE analysis for stair climbing condition

| **Stair climbing condition** | | |
|---|---|---|
| **Case** | **Forces involved** | **Location** |
| 1 | Hip force only | P0 |
| 2 | Hip force + Abductors | P1 |
| 3 | Hip force + Abductors + Vastus Lateralis | P2 |
| 4 | Hip force + Abductors + Vastus Lateralis + Vastus Medialis | P3 |

For both cases, the distal end of the femoral bone was kinematically constrained, based on Martelli, Pivonka [21].

### 3.6.1 Regions of Interests (ROIs)

Regions of interests (ROIs) are the locations where the strain values of the model were observed. For each cases, the ROIs was separated in two, namely the femoral neck region and femoral shaft region, and each region will be divided more into four quadrants, which are anterior, posterior, superior and inferior (for femoral neck region) and anterior, posterior, lateral and medial (for femoral shaft region) [15]. Elements along these quadrants had been selected and the differences in strain values between cases were recorded. Figure 3.7 and 3.8 show the elements that had been selected (from point A to B) for each quadrant in both ROIs.

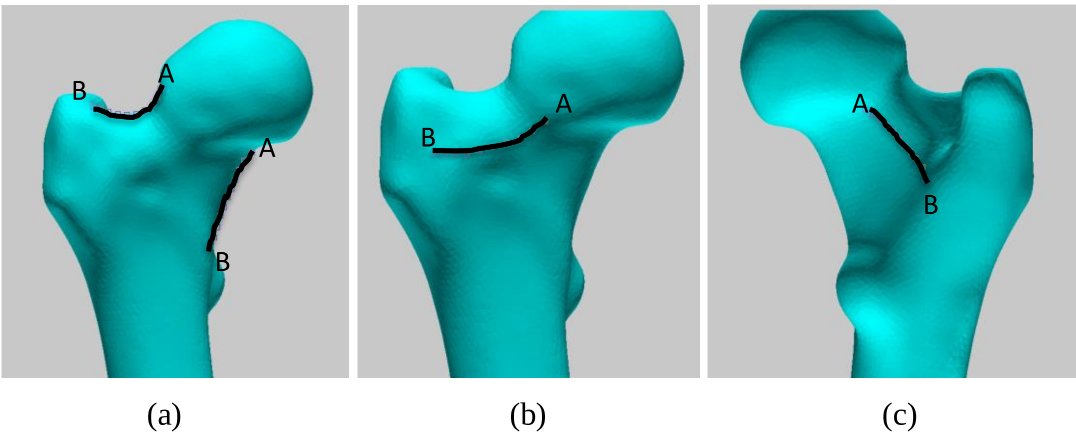


Figure 3. 7. Elements selections for (a) medial and lateral quadrants, (b) anterior quadrant and (c) posterior quadrant for femoral neck

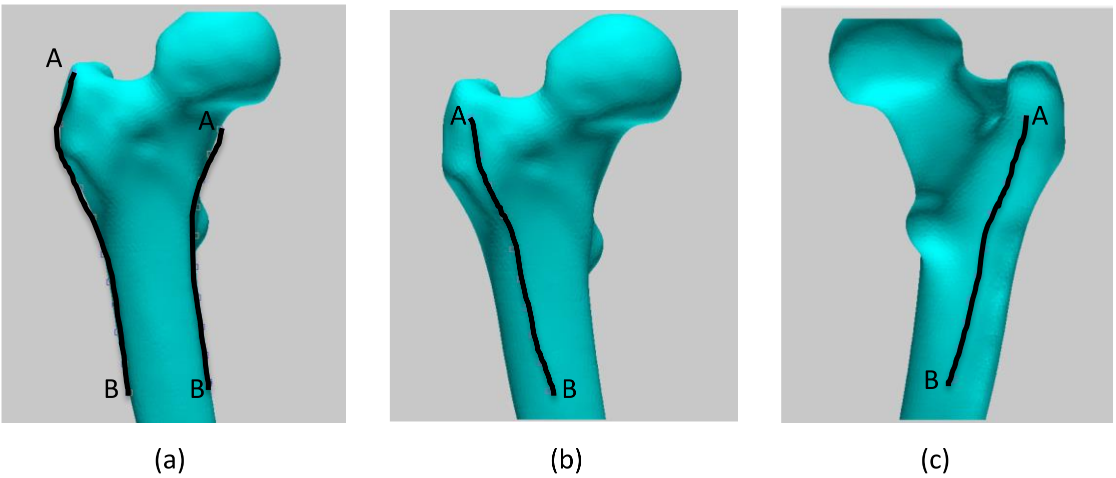


Figure 3. 8. Elements selections for (a) medial and lateral quadrants, (b) anterior quadrant, and (c) posterior quadrant for femoral shaft ROI

### 3.6.2 Strain Criterion

Strain is the amount of material deforms per unit length. Maximum principal strain was chosen to be analyzed for both conditions because of its advantages of being fairly simple, does not need calibration and well adapts to be included in the subject-specific FE models derived from CT scan [19].

# CHAPTER FOUR: RESULTS AND DISCUSSIONS

The study simulated two daily activities, namely walking and stairs climbing conditions and observed the muscles forces effects to the strain values of the femoral bone. The muscles involved for walking condition are the abductors and vastus lateralis, and for stairs climbing condition, the additional muscle of vastus medialis. Two regions of interests (ROI) were chosen as the fractures tends to occur in these sites. The ROIs are femoral neck and femoral shaft and were divided into four quadrants; inferior, superior, anterior and posterior.

## 4.1 Walking Condition

### 4.1.1 ROI – Femoral neck

Three cases of loading conditions were performed to the femoral bone for walking activity and the strain values (maximum and minimum) were recorded and compared between cases as follow (Figure 4.1). In the inferior quadrant, the maximum percentage difference is recorded between case 1 and 3 (16.28%) whereas the minimum is between case 2 and case 3 (6.64%). For the superior quadrant, the percentage difference are 21.31%, 19.64% and 2.119% between case 1 and 2, case 1 and 3 and case 2 and 3 respectively. For anterior quadrant, the highest percentage difference is between case 2 and 3 with 13.957% and the lowest is between case 1 and 3 with 0.49%. Last but not least is the posterior quadrant, where the difference of percentage between case 1 and 3 is 24.50%, the highest differences recorded for that quadrant.

### 4.1.2 ROI – Femoral shaft

Same procedure were applied to the femoral shaft region, whereby strain values of the four quadrants (medial, lateral, anterior and posterior) were recorded and compared between each cases (Figure 4.2). For medial quadrant, the maximum percentage difference obtained when case 1 is compared with case 2 (11.47%) and the minimum is between case 1 and case 3 (4.58%). In lateral quadrant, maximum percentage difference of 37.656% is obtained when case 2 is compared to case 3. For anterior quadrant, of the femoral shaft, the highest difference is between case 2 and 3 (21.032%) and the lowest is between case 1 and 3 (3.07%). The final quadrant, the posterior side, the comparison between case 1 and 2 is noted the highest, with 22.01% different.

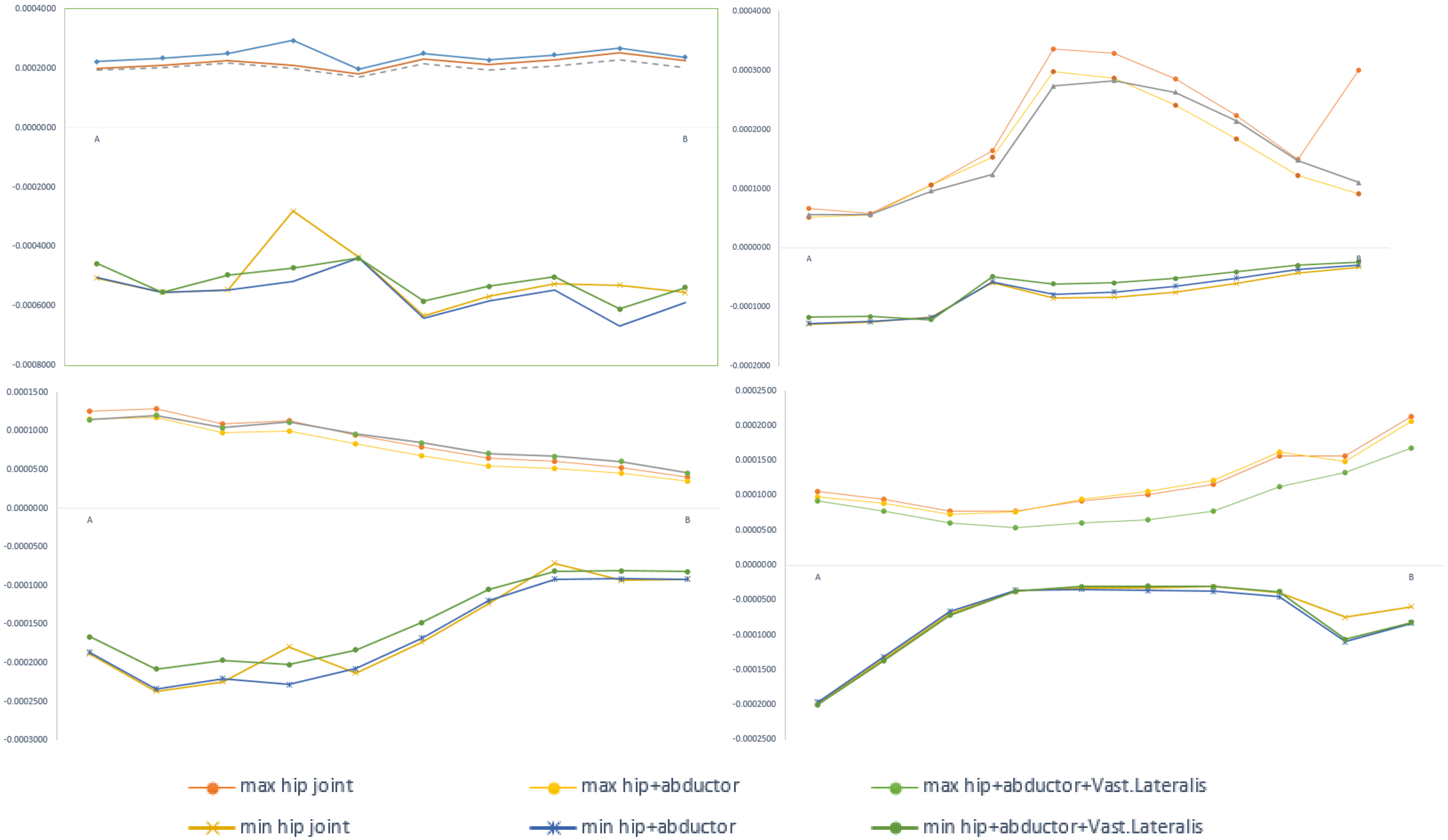


Figure 4. 1. Maximum and minimum principal strain for inferior (top left), superior (bottom left), anterior (top right) and posterior (bottom right) quadrants for femoral neck region (walking condition)

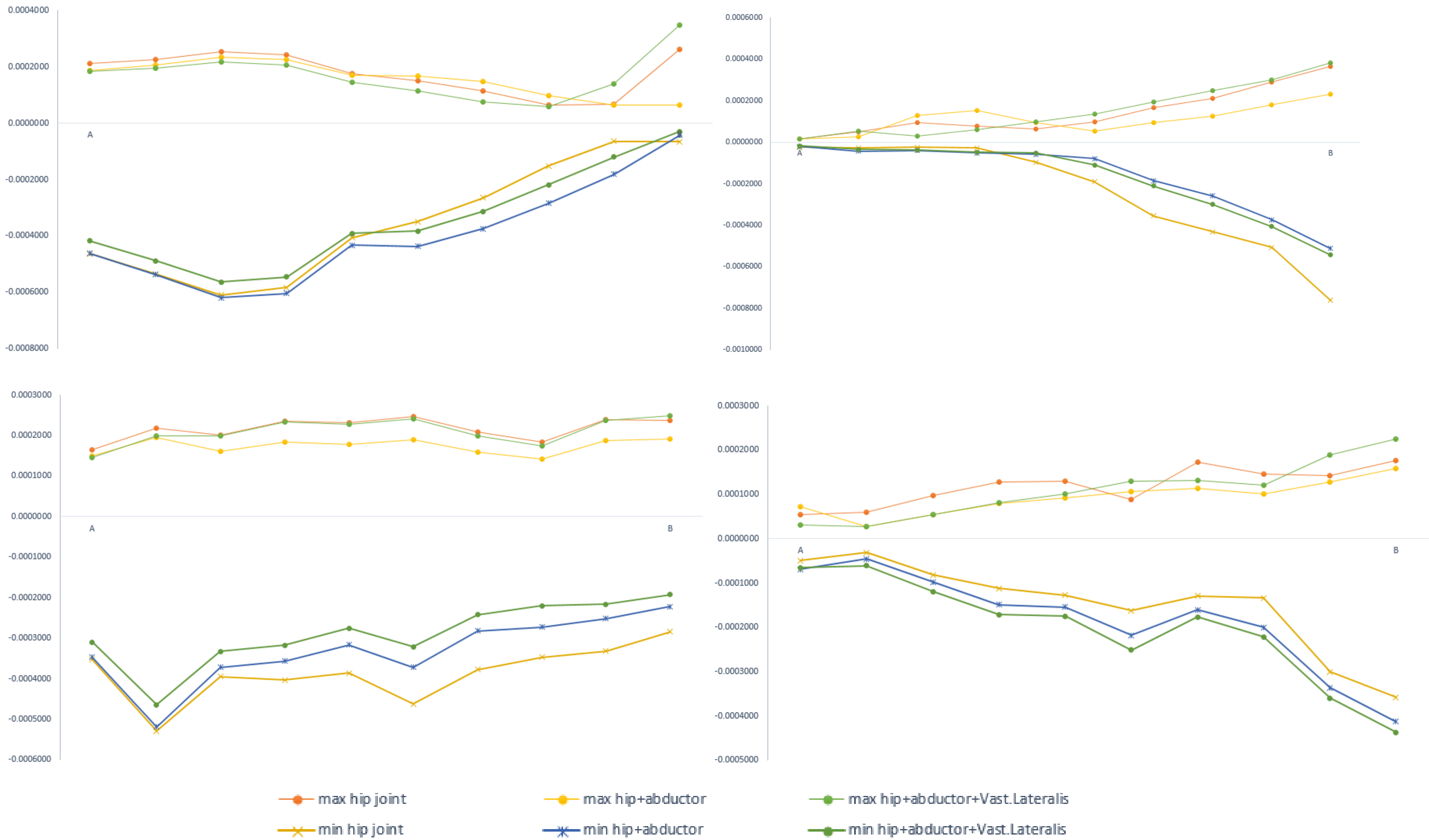


Figure 4. 2. Maximum and minimum principal strain for medial (top left), lateral (bottom left), anterior (top right) and posterior (bottom right) quadrants for femoral shaft region (walking condition)